

Effects of quantum quench on entanglement dynamics in antiferromagnetic Ising model

Yue Li(李玥), Panpan Fang(房盼盼), Zhe Wang(王哲), Panpan Zhang(张盼盼), Yuliang Xu(徐玉良), and Xiangmu Kong(孔祥木)

Citation: Chin. Phys. B, 2023, 32 (**10**): 100303. DOI: 10.1088/1674-1056/ace15c
Journal homepage: http://cpb.iphy.ac.cn; http://iopscience.iop.org/cpb

What follows is a list of articles you may be interested in

Entanglement properties of superconducting qubits coupled to a semi-infinite transmission line

Yang-Qing Guo(郭羊青), Ping-Xing Chen(陈平形), and Jian Li(李剑)
Chin. Phys. B, 2023, 32 (**6**): 060302. DOI: 10.1088/1674-1056/acc0fa

Generation of microwave photon perfect *W* states of three coupled superconducting resonators

Xin-Ke Li(李新克), Yuan Zhou(周原), Guang-Hui Wang(王光辉), Dong-Yan Lv(吕东燕),Fazal Badshah, and Hai-Ming Huang(黄海铭)
Chin. Phys. B, 2023, 32 (**4**): 040306. DOI: 10.1088/1674-1056/aca394

Characterizing entanglement in non-Hermitian chaotic systems via out-of-time ordered correlators

Kai-Qian Huang(黄恺芊), Wei-Lin Li(李蔚琳), Wen-Lei Zhao(赵文垒), and Zhi Li(李志)
Chin. Phys. B, 2022, 31 (**9**): 090301. DOI: 10.1088/1674-1056/ac67c3

Effects of colored noise on the dynamics of quantum entanglement of a one-parameter qubit—qutrit system

Odette Melachio Tiokang, Fridolin Nya Tchangnwa, Jaures Diffo Tchinda,Arthur Tsamouo Tsokeng, and Martin Tchoffo
Chin. Phys. B, 2022, 31 (**5**): 050306. DOI: 10.1088/1674-1056/ac2f36

Influences of spin-orbit interaction on quantum speed limit and entanglement of spin qubits in coupled quantum dots

M Bagheri Harouni
Chin. Phys. B, 2021, 30 (**9**): 090301. DOI: 10.1088/1674-1056/abeef4

Effects of quantum quench on entanglement dynamics in antiferromagnetic Ising model

Yue Li(李玥)[1], Panpan Fang(房盼盼)[1,2], Zhe Wang(王哲)[1,2], Panpan Zhang(张盼盼)[1,3], Yuliang Xu(徐玉良)[1], and Xiangmu Kong(孔祥木)[1,2,†]

[1] *School of Physics and Optoelectronic Engineering, Institute of Theoretical Physics, Ludong University, Yantai* 264025, *China*
[2] *College of Physics and Engineering, Qufu Normal University, Qufu* 273165, *China*
[3] *Department of Physics, Beijing Normal University, Beijing* 100875, *China*

(Received 14 April 2023; revised manuscript received 11 June 2023; accepted manuscript online 25 June 2023)

We study the relationship between quench dynamics of entanglement and quantum phase transition in the antiferromagnetic Ising model with the Dzyaloshinskii–Moriya (DM) interaction by using the quantum renormalization-group method and the definition of negativity. Two types of quench protocols (i) adding the DM interaction suddenly and (ii) rotating the spins around x axis are considered to drive the dynamics of the system, respectively. By comparing the behaviors of entanglement in both types of quench protocols, the effects of quench on dynamics of entanglement are studied. It is found that there is the same characteristic time at which the negativity firstly reaches its maximum although the system shows different dynamical behaviors. Especially, the characteristic time can accurately reflect the quantum phase transition from antiferromagnetic to saturated chiral phases in the system. In addition, the correlation length exponent can be obtained by exploring the nonanalytic and scaling behaviors of the derivative of the characteristic time.

Keywords: quantum entanglement, quantum phase transition, quantum quench, quantum renormalization group

PACS: 03.65.Ud, 73.43.Nq, 05.70.Ln, 03.67.Mn **DOI:** 10.1088/1674-1056/ace15c

1. Introduction

Due to nonclassical correlation properties of quantum entanglement, it has been widely applied in quantum information and computation.[1–8] Nowadays, it has been accepted as a useful tool to describe some important physical phenomena in quantum spin systems, such as quantum phase transition (QPT) which occurs at zero temperature and is driven by quantum fluctuation.[9–16] The equilibrium properties of quantum entanglement and QPT have been extensively studied in some spin systems.[17,18] One of the most representative work is that Osterloh *et al.* investigated the concurrence in the one-dimensional XY model with a transverse magnetic field and found that the entanglement plays an important role in the detection of QPT.[11] Then the Ising, XY and XXZ spin chains were studied by the quantum renormalization-group (QRG) method, and it is found that the first derivatives of the entanglements show the scaling behaviors close to the quantum critical points of these models.[19–26]

In recent years, with the advances in experiments of ultracold atom, the dynamical evolution of the spin system has become a frontier problem in the field of condensed matter physics.[27–33] Quantum quench is a typical method which can drive the dynamics of the spin system, and up to now most of the attentions have been devoted to the dynamical quantities following sudden quench.[34–43] In 2013, Karrasch *et al.* applied the matrix product state method to study three types of Ising models in the presence of two additional terms which break integrability, and they found that the rate functions for the return probability to the initial state in all of the Ising models become a nonanalytic function of time in the thermodynamic limit.[37] In 2014, Hazzard *et al.* investigated the time evolution of quantum correlation and entanglement following three types of quantum quench protocols which are initiated from uncorrelated states that are easily prepared in the experiment using complementary analytic and numerical methods.[38]

However, there are still some open questions in the dynamics of quantum spin systems: How is the relation between entanglement and QPT in quantum quench protocol? Especially, if we adopt both types of quench protocols, what are the different behaviors of entanglement? Does the scaling behavior of entanglement exist? To answer these questions, we study the dynamics of entanglement and QPT in the antiferromagnetic (AF) Ising model with Dzyaloshinskii–Moriya (DM) interaction in both types of quench protocols. The manuscript is organized as follows: The model and QRG method are introduced in Section 2. We analyze the dynamical behavior of entanglement near the critical point In Section 3. Then the nonanalytic and scaling behaviors of the time are discussed in Section 4. We summarize our results in Section 5.

[†]Corresponding author. E-mail: kongxm668@163.com

© 2023 Chinese Physical Society and IOP Publishing Ltd

2. Model and method

The Hamiltonian of one-dimensional AF Ising model with DM interaction in the z direction on a periodic chain of L sites can be written as

$$H_0 = \frac{J}{4}\sum_i^L \left[\sigma_i^z\sigma_{i+1}^z + D\left(\sigma_i^x\sigma_{i+1}^y - \sigma_i^y\sigma_{i+1}^x\right)\right], \tag{1}$$

where σ_i^α ($\alpha = x,y,z$) are Pauli matrices on the i-th site.[44–46] The parameter $J>0$ denotes the AF coupling and D is the reduced parameter which is related to DM interaction.

Next, we apply the QRG method to discuss the properties of the above system.[47–49] This method not only simplifies the degree of freedom of the system, but also maintains the invariance of the low-energy spectrum, which is very important for exploring quantum problems at zero temperature. A brief introduction to the steps of QRG is following. The Hamiltonian of the system is divided into block Hamiltonian and interblock one. The Hamiltonian of each block is diagonalized exactly, and the double degenerate ground states are kept to construct the basis for renormalized Hilbert space. Then the Hamiltonian is projected onto the renormalized space, and the effective Hamiltonian is obtained. However, the effective Hamiltonian is not exactly similar to the initial one, that is, the sign of DM interaction is changed. To have a self-similar Hamiltonian, we implement a π rotation around x axis on all sites.[23,50] The Hamiltonian H_0 is transformed to

$$H = \frac{J}{4}\sum_i^L \left[\sigma_i^z\sigma_{i+1}^z - D\left(\sigma_i^x\sigma_{i+1}^y - \sigma_i^y\sigma_{i+1}^x\right)\right]. \tag{2}$$

The specific transformation steps are as follows. Considering three sites as a block, the Hamiltonian can be written as $H = H^{\mathrm{B}} + H^{\mathrm{BB}}$, where H^{B} and H^{BB} are the block Hamiltonian and interblock one, respectively,

$$H^{\mathrm{B}} = \sum_k^{L/3} H_k^{\mathrm{B}}, \tag{3}$$

$$H^{\mathrm{BB}} = \frac{J}{4}\sum_k^{L/3}\left[\sigma_{k,3}^z\sigma_{k+1,1}^z - D\left(\sigma_{k,3}^x\sigma_{k+1,1}^y - \sigma_{k,3}^y\sigma_{k+1,1}^x\right)\right], \tag{4}$$

where

$$\begin{aligned} H_k^{\mathrm{B}} = \frac{J}{4}\Big[&\sigma_{k,1}^z\sigma_{k,2}^z + \sigma_{k,2}^z\sigma_{k,3}^z \\ &- D\left(\sigma_{k,1}^x\sigma_{k,2}^y - \sigma_{k,1}^y\sigma_{k,2}^x + \sigma_{k,2}^x\sigma_{k,3}^y - \sigma_{k,2}^y\sigma_{k,3}^x\right)\Big]. \end{aligned} \tag{5}$$

The two degenerate ground states of the three-site block Hamiltonian H_k^{B} in the space spanned by $\{|\uparrow\uparrow\uparrow\rangle, |\uparrow\uparrow\downarrow\rangle, |\uparrow\downarrow\uparrow\rangle, |\uparrow\downarrow\downarrow\rangle, |\downarrow\uparrow\uparrow\rangle, |\downarrow\uparrow\downarrow\rangle, |\downarrow\downarrow\uparrow\rangle, |\downarrow\downarrow\downarrow\rangle\}$ (where $|\uparrow\rangle$ and $|\downarrow\rangle$ denote the eigenstates of σ^z) can be obtained as

$$|\varphi_0\rangle = -\frac{1}{\sqrt{\lambda^2+2}}\left(|\uparrow\uparrow\downarrow\rangle - \lambda|\uparrow\downarrow\uparrow\rangle - |\downarrow\uparrow\uparrow\rangle\right), \tag{6a}$$

$$|\varphi_0'\rangle = -\frac{1}{\sqrt{\lambda^2+2}}\left(|\uparrow\downarrow\downarrow\rangle - \lambda|\downarrow\uparrow\downarrow\rangle - |\downarrow\downarrow\uparrow\rangle\right), \tag{6b}$$

where

$$\lambda = \frac{1+\mu}{2D},\ \mu = \sqrt{1+8D^2}. \tag{7}$$

The projection operator of the ground state is defined as $P_0 = \prod_{k=1}^{L/3} P_0^k$, where $P_0^k = |\Uparrow\rangle\langle\varphi_0| + |\Downarrow\rangle\langle\varphi_0'|$, in which the $|\varphi_0\rangle$ and $|\varphi_0'\rangle$ are the two degenerate ground states of H_k^{B}, and the $|\Uparrow\rangle$ and $|\Downarrow\rangle$ are the renamed states of the k-th block in effective Hilbert space. The effective Hamiltonian can be obtained by applying the projection operator to H, that is,

$$H^{\mathrm{eff}} = P_0 H P_0^\dagger = P_0 H^{\mathrm{B}} P_0^\dagger + P_0 H^{\mathrm{BB}} P_0^\dagger. \tag{8}$$

By $P_0\sigma_{k,i}^\alpha P_0^\dagger = \xi_{k,i}^\alpha \sigma_k'^\alpha$, the Pauli matrices have the following transformations

$$P_0\sigma_{k,1}^x P_0^\dagger = \frac{2D}{\mu}\sigma_k'^y,\quad P_0\sigma_{k,3}^x P_0^\dagger = -\frac{2D}{\mu}\sigma_k'^y, \tag{9}$$

$$P_0\sigma_{k,1}^y P_0^\dagger = -\frac{2D}{\mu}\sigma_k'^x,\quad P_0\sigma_{k,3}^y P_0^\dagger = \frac{2D}{\mu}\sigma_k'^x, \tag{10}$$

$$P_0\sigma_{k,1}^z P_0^\dagger = \frac{1+\mu}{2\mu}\sigma_k'^z,\quad P_0\sigma_{k,3}^z P_0^\dagger = \frac{1+\mu}{2\mu}\sigma_k'^z. \tag{11}$$

The effective Hamiltonian is obtained by bringing the above formula into Eq. (8). For the request of QRG method is that the effective Hamiltonian has a similar structure to the initial one, the effective Hamiltonian is expressed as

$$H^{\mathrm{eff}} = \frac{J'}{4}\sum_i^L \left[\sigma_i^z\sigma_{i+1}^z - D'\left(\sigma_i^x\sigma_{i+1}^y - \sigma_i^y\sigma_{i+1}^x\right)\right], \tag{12}$$

where

$$J' = J\left(\frac{1+\mu}{2\mu}\right)^2,\ D' = \frac{16D^3}{(1+\mu)^2}. \tag{13}$$

By analyzing Eq. (13), the fixed points are obtained by only solving $D' = D$. The stable fixed points locate at $D = 0,\infty$, and the unstable fixed point (the critical point) locates at $D = 1$. Under QRG iterations, the coupling constant D goes to zero for $D<1$ and infinity for $D>1$. At the stable fixed point $D=0$, the ground state of the system is AF phase (Néel phase). With the increasing of the DM interaction, the quantum fluctuation destroys the AF order in z direction and gradually makes spins to be oriented in the "XY plane". The QPT happens at the critical point $D_{\mathrm{c}} = 1$. For $D>1$, the system represents a saturated chiral phase.[23]

3. Dynamical behavior of entanglement

In order to study the dynamical behavior of entanglement near the critical point, we adopt the negativity to measure the

ground-state entanglement between two sites. The density matrix of the system consisting of two subsystems is positive definite, and the density matrix can be written in the direct product form ($\rho = \rho_1 \otimes \rho_2$) for the separable states. In this case, the partial transposition density matrix is still a non-negative separable matrix $\left(\rho^{T_1} = \rho_1^T \otimes \rho_2\right)$, and its eigenvalues are all positive, otherwise, the system is in the entangled state.[51] Therefore, the negativity is defined as

$$N(\rho) = \sum_i |u_i|, \tag{14}$$

where u_i are the negative eigenvalues of the partial transposition density matrix, and ρ is the density matrix for the system of two sites.[52]

Next, we investigate the time evolution of the entanglement by considering two types of quench protocols (i) adding the DM interaction suddenly and (ii) rotating π around x axis on all sites to drive the dynamics of the system.

Quench protocol (i): The system starts with one of the two degenerate ground states of the pure Ising Hamiltonian

$$H_1 = \frac{J}{4}\sum_i^L \sigma_i^z \sigma_{i+1}^z, \tag{15}$$

and then make the Hamiltonian change abruptly to H at $t = 0$ to realize quench. In order to apply the QRG method to calculate the entanglement in a large system, we firstly consider a three-spin system. The initial density matrix for this system is $\rho(0) = |\psi_0\rangle\langle\psi_0|$, where $|\psi_0\rangle = |\uparrow\downarrow\uparrow\rangle$ is one of the degenerate ground states of the Hamiltonian (three-spin case)

$$H_{01} = \frac{J}{4}\left(\sigma_1^z\sigma_2^z + \sigma_2^z\sigma_3^z\right). \tag{16}$$

The DM interaction is added at $t = 0$, suddenly, and the density matrix for three-spin system at time t can be obtained by $\rho(t) = U(t)\rho(0)U^\dagger(t)$, where $U(t) = \mathrm{e}^{-\mathrm{i}Ht}$ is the evolution operator

$$U(t) = \begin{pmatrix} u & 0 & 0 & 0 & 0 & 0 & 0 & 0 \\ 0 & v & -x & 0 & w & 0 & 0 & 0 \\ 0 & x & 0 & 0 & -x & 0 & 0 & 0 \\ 0 & 0 & y & v & 0 & -x & w & 0 \\ 0 & w & x & 0 & v & 0 & 0 & 0 \\ 0 & 0 & 0 & x & 0 & y & -x & 0 \\ 0 & 0 & 0 & w & 0 & x & v & 0 \\ 0 & 0 & 0 & 0 & 0 & 0 & 0 & u \end{pmatrix}, \tag{17}$$

in which

$$\begin{aligned} u &= \mathrm{e}^{-\mathrm{i}Jt/2}, \\ v &= \frac{1+\mathrm{e}^{\mathrm{i}Jt/4}\left(\cos(\mu Jt/4) - \frac{\sinh(\mathrm{i}\mu Jt/4)}{\mu}\right)}{2}, \\ w &= \frac{1-\mathrm{e}^{\mathrm{i}Jt/4}\left(\cos(\mu Jt/4) - \frac{\sinh(\mathrm{i}\mu Jt/4)}{\mu}\right)}{2}, \end{aligned}$$

$$\begin{aligned} x &= \frac{2D\mathrm{e}^{\mathrm{i}Jt/4}\sinh(\mathrm{i}\mu Jt/4)}{\mu}, \\ y &= \frac{\mathrm{e}^{\mathrm{i}Jt/4}\left[\mu^2\cos(\mu Jt/4) + \mu\sinh(\mathrm{i}\mu Jt/4)\right]}{\mu}. \end{aligned}$$

Without loss of generality, we trace over the spin 2 and calculate the pairwise entanglement of spins 1 and 3. The reduced density matrix for spins 1 and 3 can be obtained as

$$\rho_{13} = \begin{pmatrix} m & 0 & 0 & 0 \\ 0 & -n & n & 0 \\ 0 & n & -n & 0 \\ 0 & 0 & 0 & 0 \end{pmatrix}, \tag{18}$$

where

$$\begin{aligned} m &= \frac{1+4D^2+4D^2\cos(\mu Jt/2)}{\mu^2}, \\ n &= \frac{4D^2\sinh(\mathrm{i}\mu Jt/4)^2}{\mu^2}. \end{aligned} \tag{19}$$

According to Eq. (14), the negativity for sites 1 and 3 is obtained as

$$N_1(t) = (a_1 - b_1)/2\mu, \tag{20}$$

where

$$\begin{aligned} a_1 &= \sqrt{\mu^2 + 48D^4 + 8D^2\cos(\mu Jt/2) + 16D^4\cos(\mu Jt)}, \\ b_1 &= 1 + 4D^2 + 4D^2\cos(\mu Jt/2). \end{aligned} \tag{21}$$

Supposing $J = 1$, the negativity $N_1(t)$ versus time t for $D = 0.9$, 1.0 and 1.1 is shown in Fig. 1. It is found that the negativity starts from zero and oscillates periodically over the time whatever $D = 0.9$, 1.0 or 1.1. This is due to that the initial pure Ising state is separable such that the negativity equals zero, and the AF order competing with saturated chiral order. The variation of the entanglement on left side of the critical point ($D = 0.9$) is different from that of the right ($D = 1.1$). As the length of the chain increases, the amplitude of $N_1(t)$ decreases gradually and finally vanishes when the quench occurs at $D = 0.9$ in Fig. 1(a). The reason for this is that AF phase plays a main role when the coupling constant D goes to zero with QRG iterations. Conversely, the amplitude of $N_1(t)$ in Fig. 1(c) increases gradually as the size of the system becomes large when the quench occurs at $D = 1.1$. The running of coupling constant D goes to infinity at the thermodynamic limit, and the saturated chiral order has main effect on dynamical evolution of the system. When the system is in the critical point D_c, the correlation length of quantum fluctuation is divergent, so the evolutions of $N_1(t)$ coincide with each other for different sizes of the system in Fig. 1(b).

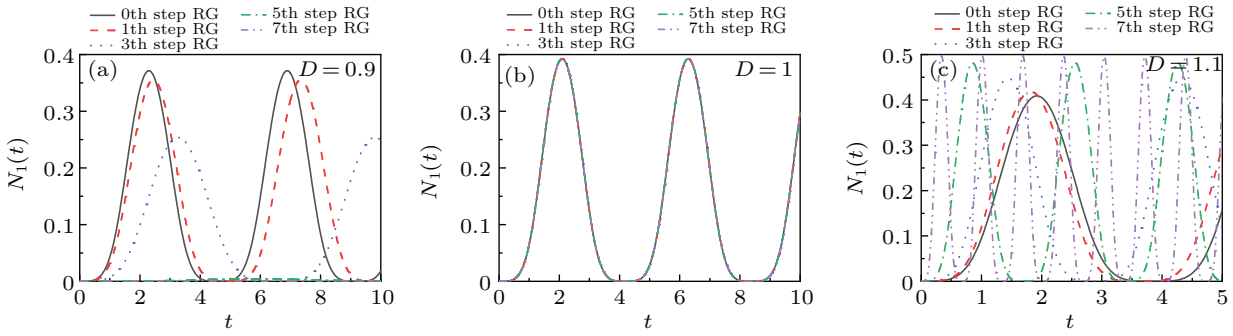


Fig. 1. The evolution of $N_1(t)$ in terms of QRG iterations versus t (where the unit of time is $1/J$) in the quench protocol (i). panel (a) corresponds to the left of critical point, panel (b) corresponds to the critical point, and panel (c) corresponds to the right of critical point.

Quench protocol (ii): Let the system start with one of the degenerate ground state of the Hamiltonian H_2 which can be written as

$$H_2 = \frac{J}{4}\sum_{i}^{L}\left[\sigma_i^z\sigma_{i+1}^z + D\left(\sigma_i^x\sigma_{i+1}^y - \sigma_i^y\sigma_{i+1}^x\right)\right], \tag{22}$$

and then the Hamiltonian is changed to H by implementing a π rotation around x axis on all sites at $t=0$. Similarly, the negativity for sites 1 and 3 can be obtained as

$$N_2(t) = (a_2 - b_2)/4\mu^3, \tag{23}$$

where

$$\begin{aligned} a_2 &= 2\sqrt{1+4D^2+192D^4+256D^6+16D\mu^2\cos(\mu Jt/2)+64D^4\cos(\mu Jt)}, \\ b_2 &= 1+\mu+8D^2(\mu-1)+16D^4\cos(\mu Jt/2). \end{aligned} \tag{24}$$

Figure 2 shows the relations of $N_2(t)$ versus t under different QRG iterations for $D=0.9$, 1.0 and 1.1. The result is far from the quench protocol (i). The entanglement starts to oscillate periodically from nonzero with time t. For $D=0.9$, the amplitude of $N_2(t)$ first increases and then decreases due to the quantum fluctuation caused by spin rotation as the size of the system becomes large and becomes zero at $L\to\infty$ when the system becomes AF order in Fig. 2(a). In the case of $D=1.1$, the amplitude of $N_2(t)$ decreases gradually and finally keeps stable because of the influence at the saturated chiral order in a large system. When $D=1.0$, the negativity of different-length chains coincides with each other in Fig. 2(b), and the physical cause is the same as the quench protocol (i).

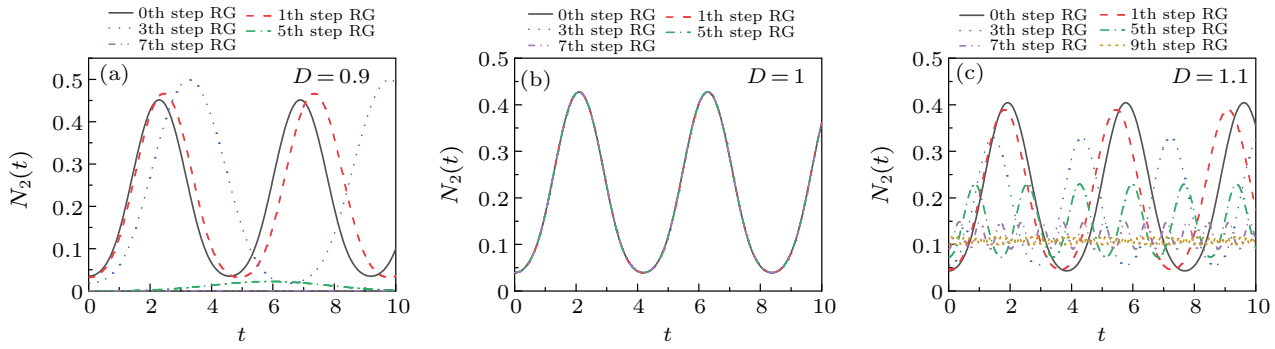


Fig. 2. The evolution of $N_2(t)$ under QRG steps versus t (where the unit of time is $1/J$) in the quench protocol (ii). Panels (a), (b), and (c) correspond to the left of critical point, the critical point, and the right of critical point, respectively.

Next, the evolutions of negativity versus D for $t=1.0$ in the quench protocols (i) and (ii) are given in Fig. 3. For the quench protocol (ii), the negativity oscillates from zero with the DM interaction in Fig. 3(a). With the length of the chain increasing, it is found that the oscillation behavior of $N_1(D)$ becomes more and more intense, and the first peak of negativity will approach to the critical point $D=1.0$. For the quench protocol (ii), the negativity starts from zero to maximum and then decreases gradually, and finally oscillates slightly at the near of a certain point with the DM interaction increasing in Fig. 3(b). The height of each peak decreases gradually and then finally decreases to a fixed value as $D\to\infty$. As the size

of the system becomes large, the first peak of the negativity also approaches to D_c. The fact shows that no matter what quench method is chosen, the entanglement always suddenly changes at the critical point.

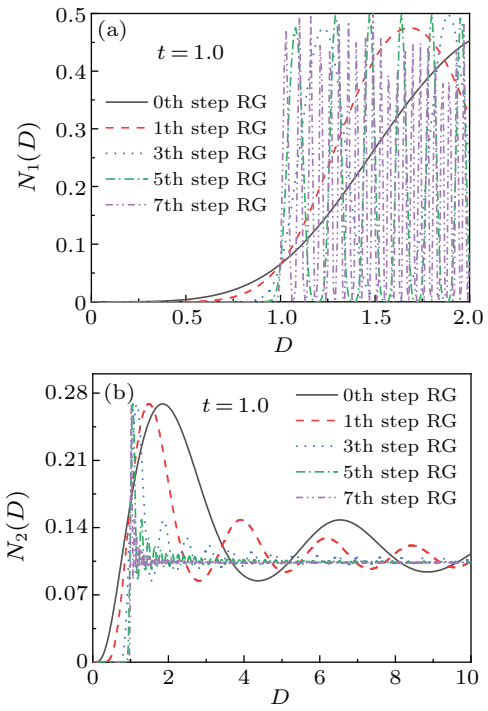


Fig. 3. The variation of $N_1(D)$ and $N_2(D)$ under QRG steps versus D when $t = 1.0$. Panels (a) and (b) correspond to both types of quench protocols (i) and (ii), respectively.

4. Nonanalytic and scaling behaviors

By analyzing the above results, we find that although the system shows different dynamical behaviors in both quench protocols (i) and (ii), there is a same characteristic time T at which the $N_1(t)$ and $N_2(t)$ firstly reach its maximum. The characteristic time T is

$$T = \frac{2\pi}{\sqrt{1+8D^2}}. \tag{25}$$

The characteristic time T versus D for different sizes of the system is given in Fig. 4. It is found that the characteristic time decreases with the increase of DM interaction. At the left side of the critical point, D gradually approaches the stable fixed point $D = 0$ with the increase of the number of QRG iterations, and T gradually increases. In the thermodynamic limit, the system is in the AF phase. At the right side of the critical point, D gradually approaches the stable fixed point $D = \infty$ with the increase of the system size, and the characteristic time gradually decreases. By increasing the size of the system, T develops two saturated values gradually at $D = 1.0$, and equation (25) becomes a discontinuous function, which reflects the quantum phase transition from antiferromagnetic to saturated chiral phases.

For understanding the phase transition deeply, the first derivatives of the time T versus D under QRG steps are shown in Fig. 5. As the size of system becomes large through QRG iterations, the first derivative of T shows a nonanalytic behavior at the critical point ($D = 1.0$) obtained in Section 2, which indicates that the first derivative of the characteristic time can accurately reflect the quantum phase transition and the characteristic time can characterize the phase transition.

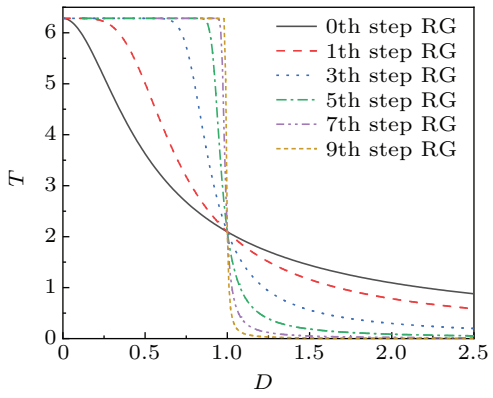


Fig. 4. The characteristic time T versus D for different QRG steps. The singular behaviors of T at the large QRG iterations correspond to the emerging of the phase transition.

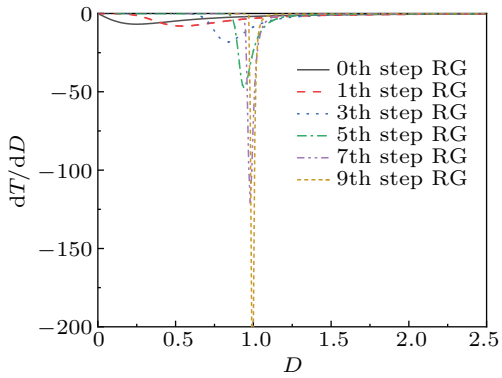


Fig. 5. The first derivative of the characteristic time T and its manifestation towards divergence as the number of QRG iterations increases.

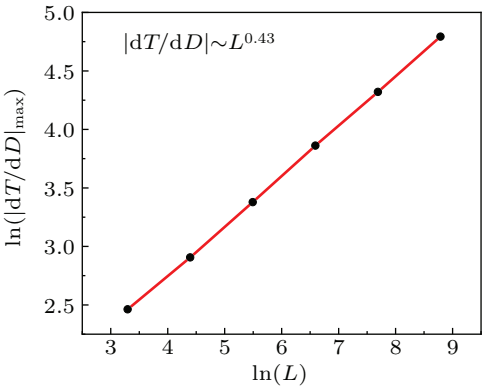


Fig. 6. The scaling behavior of the maximum for absolute value of $\mathrm{d}T/\mathrm{d}D$ versus systems of various sizes.

In order to prove the above case, we calculated the scaling behavior of the maximum of absolute value $|\mathrm{d}T/\mathrm{d}D|_{\max}$. As shown in Fig. 6, there is a linear relation between $\ln(|\mathrm{d}T/\mathrm{d}D|_{\max})$ and $\ln L$, *i.e.*, $|\mathrm{d}T/\mathrm{d}D|_{\max} \sim L^{\theta}$ with the exponent $\theta = 0.43$ (the exponent of T). The divergent behavior of correlation length in the vicinity of D_c can be written as $\xi \sim$

$|D-D_c|^{-\nu}$. After the n-th ($n=0,1,2,\ldots$) RG steps, the correlation length performs as $\xi_n=\xi/b^n$ and $\xi_n\sim|D_n-D_c|^{-\nu}$, that is, the correlation length diverges at $D_c=1.0$, where $b=3$ is the scale transformation factor. Moreover, at the critical point, $|\mathrm{d}T/\mathrm{d}D|_{D_c}\sim|\mathrm{d}D_n/\mathrm{d}D|_{D_c}$. Combining with the above formulas, the relation between the correlation length critical exponent ν and exponent θ of T can be obtained as $\theta=1/\nu$. The critical behavior of the system can be obtained by the characteristic time of the negativity, that is, the quantum phase transition can be described by the characteristic time.

5. Summary

In this manuscript, the dynamical behaviors of quantum entanglement in the Ising model with DM interaction under two types of quench protocols are studied by using QRG method. The entanglement periodically oscillates over the time for a certain DM interaction, and the variations in the amplitudes of negativity on the left side of the critical point for different QRG steps are different from that of the right in the protocol (i) or (ii). The variations of negativity with DM interaction in quench protocol (i) are different from those of the quench protocol (ii) for a certain time. It is found that the first derivative of the characteristic time can precisely reflect the quantum phase transition from antiferromagnetic to saturated chiral phases. Finally, we investigate the scaling behavior of the first derivative of T and obtain the relation between the exponents of correlation length and the characteristic time.

Acknowledgements

Project supported by the National Natural Science Foundation of China (Grant No. 11675090) and the Natural Science Foundation of Shandong Provincie, China (Grant No. ZR2022MA041). Yue Li would like to thank Li-Zhen Hu, Zhen-Hui Sun, Xiu-Ying Zhang, Qing-Hui Li, and Chuan-Zheng Miao for fruitful discussions and useful comments.

References

[1] Ekert A K 1991 *Phys. Rev. Lett.* **67** 661
[2] Horodecki R, Horodecki P, Horodecki M and Horodecki K 2009 *Rev. Mod. Phys.* **81** 865
[3] Xu X X 2015 *Phys. Rev. A* **92** 012318
[4] Wehner S, Elkouss D and Hanson R 2018 *Science* **362** 6412
[5] Cheong J W, Pradana A and Chew L Y 2022 *Phys. Rev. A* **106** 052410
[6] Mooney G J, Hill C D and Hollenberg L C L 2019 *Sci. Rep.* **9** 13465
[7] Xu Q S, Tan X Q, Huang R and Li M Q 2021 *Phys. Rev. A* **104** 042412
[8] Yang L, Liu Y C and Li Y S 2020 *Chin. Phys. B* **29** 060301
[9] Sachdev S 2011 *Quantum Phase Transitions*, 2nd edn (Cambridge: Cambridge University Press)
[10] Osborne T J and Nielsen M A 2002 *Phys. Rev. A* **66** 032110
[11] Osterloh A, Amico L, Falci G and Fazio R 2002 *Nature* **416** 608
[12] Vidal G, Latorre J I, Rico E and Kitaev A 2003 *Phys. Rev. Lett.* **90** 227902
[13] Wu L A and Sarandy M S and Lidar D A 2004 *Phys. Rev. Lett.* **93** 250404
[14] Tan X D, Jin B Q and Gao W 2013 *Chin. Phys. B* **22** 20308
[15] De Nicola S, Michailidis A A and Serbyn M 2021 *Phys. Rev. Lett.* **126** 040602
[16] Turkeshi X, Dalmonte M, Fazio R and Schirò M 2022 *Phys. Rev. B* **105** L241114
[17] Qin M, Ren Z Z and Zhang X 2018 *Chin. Phys. B* **27** 60301
[18] Zhao J H and Wang H Tao 2012 *Acta Phys. Sin.* **61** 210502 (in Chinese)
[19] Pfeuty P, Jullian R and Penson K L 1982 *Renormalization for Quantum Systems* (New York: Springer Berlin Heidelberg)
[20] Kargarian M, Jafari R and Langari A 2007 *Phys. Rev. A* **76** 060304
[21] Kargarian M, Jafari R and Langari A 2008 *Phys. Rev. A* **77** 032346
[22] Ma F W, Liu S X and Kong X M 2011 *Phys. Rev. A* **83** 062309
[23] Jafari R, Kargarian M, Langari A and Siahatgar M 2008 *Phys. Rev. B* **78** 214414
[24] Kargarian M, Jafari R and Langari A 2009 *Phys. Rev. A* **79** 042319
[25] Ma F W, Liu S X and Kong X M 2011 *Phys. Rev. A* **84** 042302
[26] Xu Y L, Kong X M, Liu Z Q and Yin C C 2017 *Phys. Rev. A* **95** 042327
[27] Bloch I, Dalibard J and Zwerger W 2008 *Rev. Mod. Phys.* **80** 885
[28] Greiner M, Mandel O, Esslinger T, Hänsch T W and Bloch I 2002 *Nature* **415** 39
[29] Sadler L E, Higbie J M, Leslie S R, Vengalattore M and Stamper-Kurn D M 2006 *Nature* **443** 312
[30] Jafari R and Akbari A 2020 *Phys. Rev. A* **101** 062105
[31] Chen J Z and Zhu J Y 2001 *Acta Phys. Sin.* **50** 1340 (in Chinese)
[32] Zhu W T, Ren Q B, Duan L W and Chen Q H 2016 *Chin. Phys. Lett.* **33** 050302
[33] Li X M, Chen Y X, Xia Y J, Zhang Q and Man Z X 2020 *Chin. Phys. B* **29** 060302
[34] Jafari R 2010 *Phys. Rev. A* **82** 052317
[35] Schachenmayer J, Lanyon B P, Roos C F and Daley A J 2013 *Phys. Rev. X* **3** 031015
[36] Alba V and Heidrich-Meisner F 2014 *Phys. Rev. B* **90** 075144
[37] Karrasch C and Schuricht D 2013 *Phys. Rev. B* **87** 195104
[38] Hazzard K R A, van den Worm M, Foss-Feig M, Manmana S R, Torre E G D, Pfau T, Kastner M and Rey A M 2014 *Phys. Rev. A* **90** 063622
[39] Cincio L, Dziarmaga J, Rams M M and Zurek W H 2007 *Phys. Rev. A* **75** 052321
[40] Mitra A 2018 *Annu. Rev. Condens. Matter Phys.* **9** 245
[41] Wang Z, Fang P P, Xu Y L, Wang C Y, Zhang R T, Zhang H and Kong X M 2021 *Physica A* **581** 126205
[42] Yan Y, Luan L N and Wang L C 2022 *Eur. Phys. J. D* **76** 146
[43] Cao K Y, Zhong M and Tong P Q 2022 *Chin. Phys. B* **31** 60505
[44] Dzyaloshinsky I 1958 *J. Phys Chem. Solids* **4** 241
[45] Moriya T 1960 *Phys. Rev.* **120** 91
[46] Picone P J, Kastner M A, Jenssen H P, Gabbe D R, Chen C Y, Birgeneau R J and Aharony A 1988 *Phys. Rev. B* **38** 905
[47] Wilson K G 1971 *Phys. Rev. B* **4** 3174
[48] Wilson K G 1971 *Phys. Rev. B* **4** 3184
[49] Wilson K G 1975 *Rev. Mod. Phys.* **47** 773
[50] Langari A 2004 *Phys. Rev. B* **69** 100402
[51] Peres A 1996 *Phys. Rev. Lett.* **77** 1413
[52] Vidal G and Werner R F 2002 *Phys. Rev. A* **65** 032314